OPEN

The Role of Lysophosphatidic Acid on Airway Epithelial Cell Denudation in a Murine Heterotopic Tracheal Transplant Model

Yukiko Tando, PhD,[1] Chiharu Ota, MD, PhD,[1] Mitsuhiro Yamada, MD, PhD,[2] Satoshi Kamata, MD, PhD,[1] Mutsuo Yamaya, MD, PhD,[1] Kuniyuki Kano, PhD,[3] Shinichi Okudaira, PhD,[3] Junken Aoki, PhD,[3,4] and Hiroshi Kubo, MD, PhD[1]

Background. Chronic rejection is the major leading cause of morbidity and mortality after lung transplantation. Obliterative bronchiolitis (OB), a fibroproliferative disorder of the small airways, is the main manifestation of chronic lung allograft rejection. However, there is currently no treatment for the disease. We hypothesized that lysophosphatidic acid (LPA) participates in the progression of OB. The aim of this study was to reveal the involvement of LPA on the lesion of OB. **Methods.** Ki16198, an antagonist specifically for LPA_1 and LPA_3, was daily administered into the heterotopic tracheal transplant model mice at the day of transplantation. At days 10 and 28, the allografts were isolated and evaluated histologically. The messenger RNA levels of LPAR in microdissected mouse airway regions were assessed to reveal localization of lysophosphatidic acid receptors. The human airway epithelial cell was used to evaluate the mechanism of LPA-induced suppression of cell adhesion to the extracellular matrix (ECM). **Results.** The administration of Ki16198 attenuated airway epithelial cell loss in the allograft at day 10. Messenger RNAs of LPA_1 and LPA_3 were detected in the airway epithelial cells of the mice. Lysophosphatidic acid inhibited the attachment of human airway epithelial cells to the ECM and induced cell detachment from the ECM, which was mediated by LPA_1 and Rho-kinase pathway. However, Ki16198 did not prevent obliteration of allograft at day 28. **Conclusions.** The LPA signaling is involved in the status of epithelial cells by distinct contribution in 2 different phases of the OB lesion. This finding suggests a role of LPA in the pathogenesis of OB.

(*Transplantation* 2015;1: e35; doi: 10.1097/TXD.0000000000000542. Published online 19 October 2015.)

Chronic rejection is the major leading cause of morbidity and mortality after lung transplantation. Obliterative bronchiolitis (OB), a fibroproliferative disorder of small airways, is the main manifestation of chronic lung allograft rejection.[1] Obliterative bronchiolitis is characterized histopathologically by the deposition of mature collagen, resulting in the occlusion of the small airways, accompanied by infiltration of inflammatory cells and proliferating fibroblasts.[2,3]

Although OB has been recognized for more than 60 years, little is known about its cellular and molecular pathogenesis. Although immunosuppression is increasingly being applied for the treatment of OB, it is not useful due to its ineffectiveness.[4] Thus, the development of a novel treatment for improving OB-related mortality is needed.

Lysophosphatidic acid (LPA) is a bioactive lipid known to regulate several cellular processes, including motility, proliferation, survival, and differentiation, by acting via G protein-coupled receptors specific to LPA.[5-7] Recently, many

studies have revealed that disturbances in normal LPA signaling may contribute to a range of diseases. These studies have implicated the potential of LPA receptor subtypes and related signaling mechanisms to provide novel therapeutic targets. In particular, LPA is involved in the onset of fibrosis in the kidney[8] and lung.[9,10]

As mentioned above, immunosuppression therapy is ineffective at the onset of OB. Thus, the investigation of another therapeutic target in OB, besides the immune system, is an important issue. Because the definitive pathology of OB is tissue fibrosis, we hypothesized that LPA participates in the progression of OB. In the present study, we aimed to investigate whether LPA contributes to the pathogenic mechanisms of OB. We used a heterotopic tracheal transplantation mouse model, which mimics the pathology of human OB,[11,12] for an in vivo pharmacological LPA signaling inhibition study. We also examined the effect of LPA on the human airway epithelial cell line, BEAS-2B.

MATERIALS AND METHODS

Animals

C3H/He and BALB/c mice were purchased from CLEA Japan. They were housed in a specific pathogen-free facility and were maintained under conditions of 12 hours light-darkness cycle and given access to food and water ad libitum. All animal experiments were approved by the Tohoku University Animal Experiment Ethics Committee and were performed in accordance with the Regulations for Animal Experiments and Related Activities at Tohoku University.

Heterotopic Tracheal Transplantation

The tracheae from donor mice were transplanted heterotopically into the subcutaneous pocket of recipient mice, as described previously.[11] In brief, 9-week-old male C3H/He donor mice were euthanized, and the tracheae were removed from donor mice via an anterior middle incision. The attached esophagus and other excess surrounding tissues were removed from the trachea. Six-week-old BALB/c mice were anesthetized with intraperitoneal ketamine cocktail (ketamine-HCl, 80 mg/kg; xylaxine-HCl, 16 mg/kg; and atropine-sulfate, 0.05 mg/kg). A trachea was implanted into a subcutaneous pocket of the recipient mouse via a small incision, which was closed with nylon sutures. Two tracheae of independent donor mouse were transplanted into 2 respective subcutaneous pockets of one recipient mouse. The grafts were harvested on days 10 and 28 after the transplantation.

In Vivo Treatment

For the inhibition of LPA receptors, an orally active LPA_1- and LPA_3-specific antagonist (Ki16198, 40 mg/kg)[13] or vehicle (12.5% dimethyl sulfoxide [DMSO] in phosphate-buffered saline [PBS]) was administered to BALB/c recipient mice before transplantation and daily for 9 or 27 days after transplantation.

Histopathology

The harvested grafts were fixed in 10% formalin. Transverse paraffin sections (3 μm thickness) were stained with hematoxylin-eosin or Elastica-Masson staining. The following 4 easily identifiable pathological processes were scored on a scale of 0 to 4 (0, normal; 1, mild; 2, moderate; 3, severe; and 4, very severe damage), as described previously[14]: (a) airway lining epithelial loss, (b) deposition of extracellular matrix (ECM), (c) leukocyte infiltration, and (d) luminal obliteration due to granulation tissue formation and/or fibrosis.

Immunohistochemistry

Paraffin sections of the grafts were deparaffinized and immersed in 0.3% H_2O_2 in methanol to inactivate endogenous peroxidase. They were then heated in Retrivagen A (pH 6.0, BD Pharmingen, San Jose, CA) for 10 minutes (for CD45 staining) or Tris-ethylenediaminetetraacetic acid, pH 9.0 (for CD31 staining). After blocking with 2% normal goat serum in PBS, the sections were incubated with an anti-CD45 antibody (6.25 μg/mL, BD Pharmingen) or anti-CD31 antibody (0.25 μg/mL, Santa Cruz, Santa Cruz, CA) at 4°C for overnight. Rat IgG (BD Pharmingen) was used for the isotype control. After incubation with the primary antibody, the sections were washed with PBS and incubated in PBS with biotinylated anti-rat IgG or anti-goat IgG (Vector Laboratories, Burlingame, CA) for 30 minutes at 30°C. The ABC method (Vector Laboratories) was performed according to the manufacturer's instruction, with 3,3′-diaminobenzidine (Dojindo Laboratories, Kumamoto, Japan) as the substrate. Quantification of vascular structure was performed using sections stained by CD31. The number of CD31 immunoreactive vascular structure located at outside of the cartilage was counted in randomly selected 50 fields from each section of vehicle- or Ki16198- treated allograft with 40 times objective lens.

Terminal Deoxynucleotidyl Transferase-Mediated Biotinylated UTP Nick-End Labeling Assay

The paraffin sections of the grafts were de-paraffinized and incubated in 0.1% sodium citrate with 0.1% Triton X-100 for 8 minutes at room temperature. Terminal deoxynucleotidyl transferase-mediated biotinylated UTP nick-end labeling (TUNEL) was accomplished using the in situ Cell Death Detection Kit, Fluorescein (Roche Applied Science, Mannheim, Germany), according to the manufacturer's instruction. After the labeling, the sections were mounted with ProLong Gold antifade reagent with 4′,6-diamidino-2-phenylindole (Life Technologies, Carlsbad, CA). The TUNEL-positive cells in the airway epithelium of the grafts were counted after the images were captured using fluorescence microscopy (BZ-9000; Keyence, Osaka, Japan).

Laser Microdissection and Quantification of Messenger RNA Levels by Real-Time Reverse Transcription-Polymerase Chain Reaction

The laser microdissection system (Laser Specifications Leica LMD6500) was used to microdissect cells from the prepared samples of native mouse trachea. From the dissected tissues, RNA was extracted and transcribed to cDNA using a GenElute Mammalian Total RNA Miniprep Kit (Sigma, St. Louis, MO) and high-capacity cDNA RT Kits (Applied Biosystems), respectively. Quantitative reverse transcription-polymerase chain reaction (PCR) was performed using Applied Biosystems 7300 Real-Time PCR System. The DNA primers used in this study were as follows:

LPA_1 fw: 5′-GAGGAATCGGGACACCATGAT, rv: 5′-ACATCCAGCAATAACAAGACCAATC, LPA_2 fw: 5′-GACCACACTCAGCCTAGTCAAGAC, rv: 5′-CTTACAGTCCAGGCCATCCA, LPA_3 fw: 5′-GCTCCCATGAAGCTAATGAAGACA, rv: 5′-AGGCCGTCCAGCAGCAGA, LPA_4 fw: 5′-CAGTGCCTCCCTGTTTGTCTTC, rv: 5′-GAGAGGGCCAGGTTGGTGAT, LPA_5 fw: 5′-AGCAACACGGAGCACA

GGTC, rv: 5′-CCAAAACAAGCAGAGGGAGGT, LPA_6 fw: 5′-CCGCCGTTTTTGTTCAGTC, rv: 5′-GAGATATGTTTT CCATGTGGCTTC and GAPDH fw: 5′-GCCAAGGTCATC CATGACAACT-3′, rv: 5′-GAGGGGCCATCCACAGTCTT-3′.

Cell Culture

BEAS-2B cells, a SV-40-transformed human bronchial epithelial cell line (European Collection of Cell Cultures, Salisbury, UK) were plated onto culture plates coated with 0.01 mg/mL fibronectin (BD Pharmingen), 0.03 mg/mL rat tail collagen type I (BD Pharmingen), and 0.01 mg/mL bovine serum albumin (Sigma) in bronchial epithelial growth medium (BEGM; Lonza, Basel, Switzerland). The cells were then cultured at 37°C in a humidified atmosphere of 5% CO_2 and 95% air.

Cell Spreading Assay

First, 24-well tissue culture plates (BD Pharmingen) were coated with 0.01 mg/mL fibronectin, 0.03 mg/mL rat tail collagen type I, and 0.01 mg/mL bovine serum albumin. Then, BEAS-2B cells (38 000 cells/well) were resuspended in BEGM with LPA (Enzo Life Sciences, Farmingdale, NY), LPA and 0.1% DMSO (Sigma), or LPA and 10 μM Ki16425 (Santa Cruz), or LPA and 10 μM Y27632 (Sigma) and were incubated on the coated plates at 37°C for 1.5 hours, respectively. Nonadherent cells were washed away with PBS, and the cells were fixed in 4% paraformaldehyde in PBS for 20 minutes at room temperature. The cells were treated with 0.1% Triton X-100 in PBS for 5 minutes, followed by staining with Alexa 546-conjugated phalloidin (Life Technologies) for 20 minutes at room temperature. After washing with PBS, the cells were mounted with Prolong Gold with 4′,6-diamidino-2-phenylindole. Images of 5 randomly selected fields in each well were captured under the fluorescence microscope, BZ-9000 (Keyence, Osaka, Japan). For the quantification of cell spreading, at least 100 adherent cells were counted. The compactness and maximum length of the cells were automatically calculated by the image processing software, TissueFAXS (Tissuegnostics, Vienna, Austria).

Cell Detachment Assay

BEAS-2B cells were incubated for 48 hours at 37°C. The media was replaced with media containing LPA and either 0.1% DMSO or 50 μM Ki16425, and the cells were further incubated at 37°C. The media with LPA and 0.1% DMSO or 50 μM Ki16425 were refreshed every 2 hours. After 6 hours, the plates were centrifuged in an inverted position at 900g for 5 minutes at 4°C. Cells remaining in the wells were then stained with 5 μg/mL Hoechst 33342 dye (Life Technologies), and the fluorescence was measured (excitation, 355 nm; emission, 460 nm) by Fluoroskan Ascent (Thermo Fisher Scientific Inc, Waltham, MA). Adherence indices were determined based on the fluorescence in the wells in which cells had been treated with LPA and DMSO or Ki16425, relative to wells in which cells had been treated with DMSO only.

Small Interfering RNA

BEAS-2B cells were seeded on the coated 6-well plate at 250,000 cells/well in the BEGM without antibiotic. After 24 hours, Cells were transfected with 20 nM of control small interfering (si)RNA (Silencer Select Negative Control 1 siRNA; Life Technologies), LPA_1 siRNA (Silencer Select Pre-designed siRNA s4451; Life Technologies), or LPA_3 siRNA (Silencer Select Pre-designed siRNA s24110; Life Technologies) using Opti-MEM I medium (Life Technologies) and Lipofectamine RNAiMAX (Life Technologies) according to the manufacturer's instruction. Cells were then incubated at 37°C for 24 hours and used for cell attachment assay.

Statistical Analysis

All results are presented as the mean ± SEM. Differences between the 2 experimental groups were analyzed for statistical significance with the Wilcoxon test or Student t test. Differences among more than 2 experimental groups were analyzed for statistical significance by 1-way analysis of variance, followed by the Tukey-Kramer test. All analyses were performed with JMP Pro version 10 software (SAS Institute Inc, Cary, NC). Differences among the groups were considered to be statistically significant at a P value less than 0.05.

RESULTS

Attenuation of Histopathology in the Heterotopically Transplanted Tracheal Allograft by an LPA_1- and LPA_3-Specific Antagonist in the Early Phase

A mouse allogeneic tracheal transplant model was used to determine the effect of an LPA_1- and LPA_3-specific antagonist, Ki16198. A tracheal segment from a C57BL/6 mouse was implanted into a subcutaneous lesion of a BALB/c mouse. Sections from the allografts were harvested 10 days after transplantation and assessed by hematoxylin-eosin (Figure 1) or Elastica-Masson staining (**Figure S1, SDC,** http://links.lww.com/TXD/A10). The loss of airway epithelial cells was observed in vehicle-treated allografts (Figures 1A, B). In contrast, epithelial cells remained in the Ki16198-treated grafts (Figures 1C, D). The histopathologic score of epithelial cell loss was significantly decreased in the Ki16198-treated grafts (Figure 1E). However, leukocyte infiltration, ECM deposition, and luminal obliteration were not changed between the vehicle and Ki16198-treated allografts (Figures 1F, G, H).

To examine whether LPA is involved in the apoptosis of airway epithelial cells at day 10, we performed the TUNEL assay on paraffin sections of allografts. As shown in Figures 2A to D, a small number of TUNEL-positive epithelial cells were observed in the Ki16198-treated allograft sections compared with the vehicle-treated sections. The average number of TUNEL-positive epithelial cells per section was significantly decreased in the Ki16198-treated group (Figure 2E).

Messenger RNAs for LPA Receptors are Expressed in the Mouse Airway Epithelial Cells

Ki16198 antagonizes both LPA_1 and LPA_3. Thus, to investigate the localization of LPA receptors in the native mouse airway epithelia, we quantified the messenger (m)RNA level of LPA receptors by a combination of laser microdissection and quantitative reverse transcription-PCR (Figure 3A). Among the 6 LPA receptors, LPA_1, LPA_2, LPA_3, and LPA_6 were expressed in the airway epithelial cells (Figures 3B, C, D, G). The mRNAs for LPA_4 and LPA_5 were hardly detected (Figures 3E, F).

### Inhibition of Airway Epithelial Cell Spreading by LPA

Our experiment using the heterotopic tracheal transplantation model harvested at day 10 showed that LPA is involved in the loss of airway epithelial cells. In addition, the mRNA of LPA_1 and LPA_3 were expressed in the airway
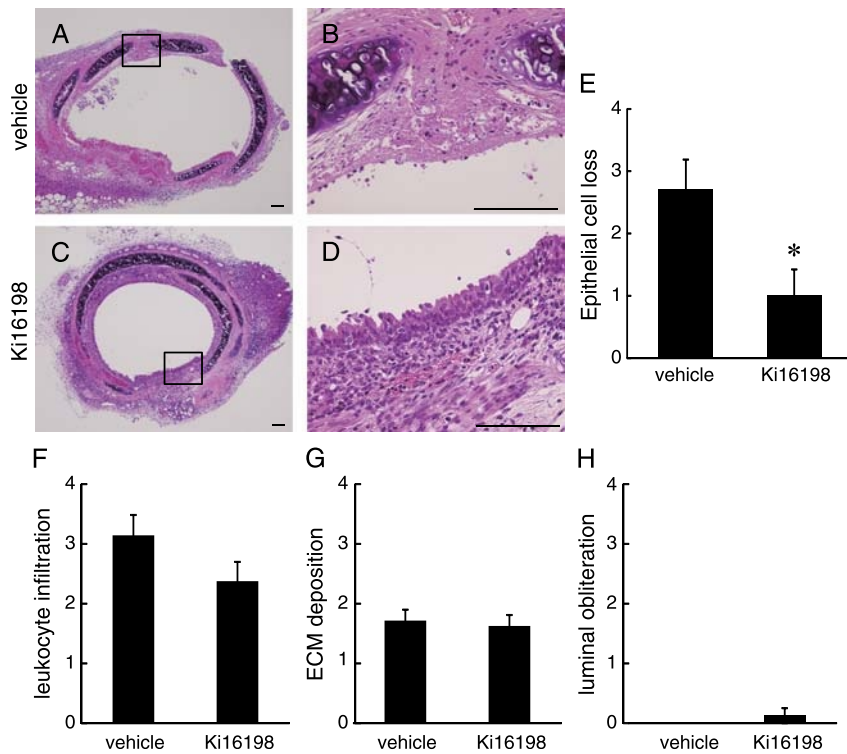
FIGURE 1. The graft histology of vehicle or Ki16198-treated mouse on day 10. A-D, Representative hematoxylin-eosin staining of the transverse section of vehicle or Ki16198-treated mouse tracheal heterotopic transplanted allograft at 10 days. The graft from a vehicle-treated mouse (A, B) shows destruction of the lining epithelium. The epithelium was maintained in the graft from a Ki16198-treated mouse (C, D). The areas surrounded by squares in panels A and C are magnified in panels B and D, respectively. Bars = 100 μm. E, The histopathologic score (0 = normal, 1 = mild, 2 = moderate, 3 = severe, and 4 = very severe damage) of the vehicle- or Ki16198-treated mouse tracheal epithelial cell loss (E), leukocyte infiltration (F), ECM deposition (G), and luminal obliteration (H). The data are expressed as the mean + SEM (n = 7 for vehicle, n = 8 for Ki16198). The data are expressed as the mean + SEM (n = 7 for vehicle, n = 8 for Ki16198), *$P < 0.05$.

epithelial cells. Therefore, we assessed the direct effect of LPA on the airway epithelial cell, BEAS-2B, which have been reported to express LPA_1 and LPA_3.[15] First, we examined the effect of LPA on cell adhesion in BEAS-2B cells. In the absence of LPA, BEAS-2B cells showed a flattened shape, with actin stress fiber formation after 1.5 hours of incubation on the coated tissue culture plate (Figures 4A, C). In contrast, the cells incubated with 1 μM of LPA showed a round shape and no stress fiber formation (Figures 4B, D). To quantify this phenomenon, we captured the images of cells stained by phalloidin, and analyzed these images by TissueFAXS software. As shown in Figure 4E, the average cell compactness was 0.27. However, this average was 0.38 in the presence of 1 μM of LPA, and the peak of histogram shifted to the
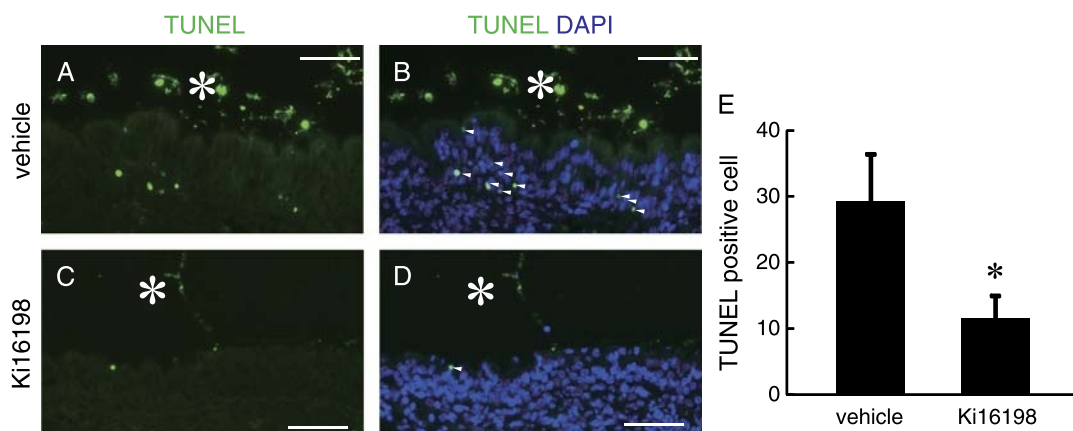
FIGURE 2. The TUNEL assay of vehicle- or Ki16198-treated mouse allografts on day 10. A-D, Representative TUNEL staining images of the transverse sections of vehicle-treated (A, B) or Ki16198-treated (C, D) mouse tracheal heterotopic transplanted allografts at 10 days. The same area of the TUNEL staining images (A, C) is merged with 4', 6-diamidino-2-phenylindole (B, D). The arrowheads indicate TUNEL-positive nucleus. The asterisks indicate the lumen of the trachea. Bars = 50 μm. E, The average of the number of TUNEL-positive cells in a section. The number of TUNEL-positive cells was decreased in the Ki16198-treated allografts compared with the vehicle-treated grafts. The data are expressed as the mean + SEM (n = 4 for vehicle; n = 8 for Ki16198), *$P < 0.05$.
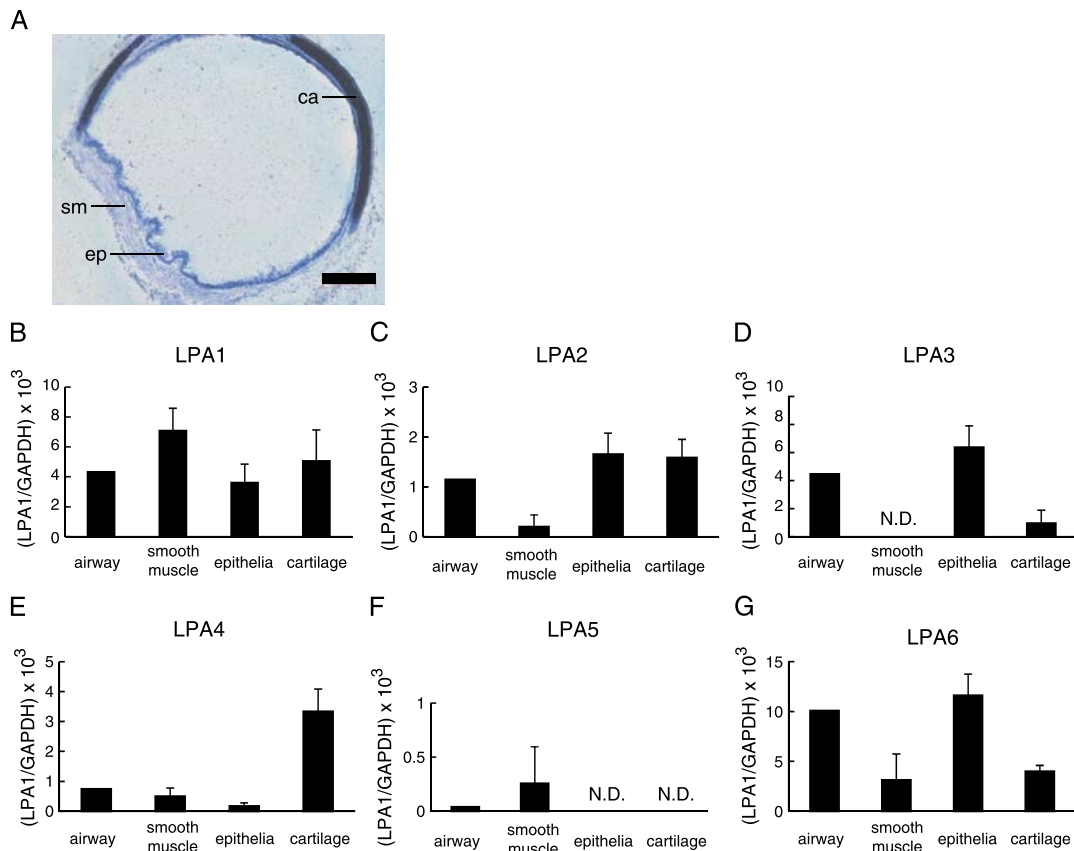
FIGURE 3. The mRNAs of LPA receptors in normal mouse airway epithelial cells. A, Transverse sections of mouse airway stained with toluidine blue. Smooth muscle (sm), epithelia (ep), and cartilage (ca) were dissected. Bar = 200 μm. B-G, Relative mRNA level of LPA_1-LPA_6. The data are expressed as the mean + SD (n = 1 for airway, n = 2 for smooth muscle, epithelia, and cartilage).

value of "1," indicating that the cells appeared more round than the cells without LPA treatment (Figure 4F). We also examined the maximum length of the cells. Compared with the histogram of maximum length without LPA, the peak of the histogram shifted to the left side in the presence of 1 μM of LPA, indicating that the cells were smaller than those without LPA (Figures 4G, H). These results indicate that LPA inhibits the spreading of BEAS-2B cells. The effects of LPA on both cell compactness and maximum length were detected at a minimum LPA concentration of 1 μM (Figures 4I, J).

To inhibit LPA signaling through LPA receptors in the attachment assay, we used another LPA_1 and LPA_3 selective antagonist, Ki16425,[16] which is effective in vitro. The cells did not spread in the presence of LPA (Figures 5B, E) compared with the absence of LPA (Figures 5A, D). However, the addition of Ki16425 with LPA restored the spreading property of the cells (Figures 5C, F). Cell compactness, which was increased by 1 μM of LPA, was significantly decreased by Ki16425 (Figure 5G). In addition, the maximum cell length was increased with Ki16425 to the same level without LPA (Figure 5H). These results indicate that LPA inhibits the spreading of BEAS-2B cells through its receptors, LPA_1 and/or LPA_3.

Induction of Airway Epithelial Cell Detachment by LPA

The effect of LPA on the attached BEAS-2B cells was evaluated. In the absence of LPA, the cells were attached to the culture plate and showed an extended morphology after 6 hours of incubation (Figure 6A). The LPA treatment diminished cell spreading, and the shape of the cells became round

(Figure 6B). Ki16425 attenuated this LPA-induced change in cell shape and detachment (Figure 6C). As shown in Figure 6D, the cell attachment ratio was decreased by LPA treatment, and Ki16425 abrogated the effect of LPA.

Involvement of LPA_1 and Rho-kinase in BEAS-2B Cell Attachment Regulation by LPA

Ki16425 treatment recovered the decreased attachment of BEAS-2B cell to the tissue culture plate. Therefore, next we downregulated LPA_1 or LPA_3 expression using siRNA to reveal which LPA receptor is dominant in this phenomena. The siRNA transfection resulted in a marked reduction of the expression of LPA_1 mRNA (Figure 7A) or LPA_3 mRNA (Figure 7B) without significant change in the expression of another LPA receptor, respectively. Then, we evaluated cell attachment using these transfected cells in the cell spreading assay. The value of compactness of the cells after transfection of siRNA for LPA_1 did not increase compared with the nontarget siRNA or LPA_3 siRNA in the presence of 1 μM LPA (Figure 7C). Furthermore, the maximum cell length did not significantly decreased compared with nontarget siRNA or LPA_3 siRNA in the presence of LPA (Figure 7D). These results indicate that LPA_1, but not LPA_3 is dominant for the cell attachment regulation by LPA. Next, we examined what kind of intracellular signaling is involved in the cell attachment regulation by LPA. We added Y27632, a Rho-associated coiled coil–forming kinase inhibitor in the presence of 1 μM LPA. As shown in Figure 7E, cell compactness, which was increased by 1 μM of LPA, was significantly decreased by
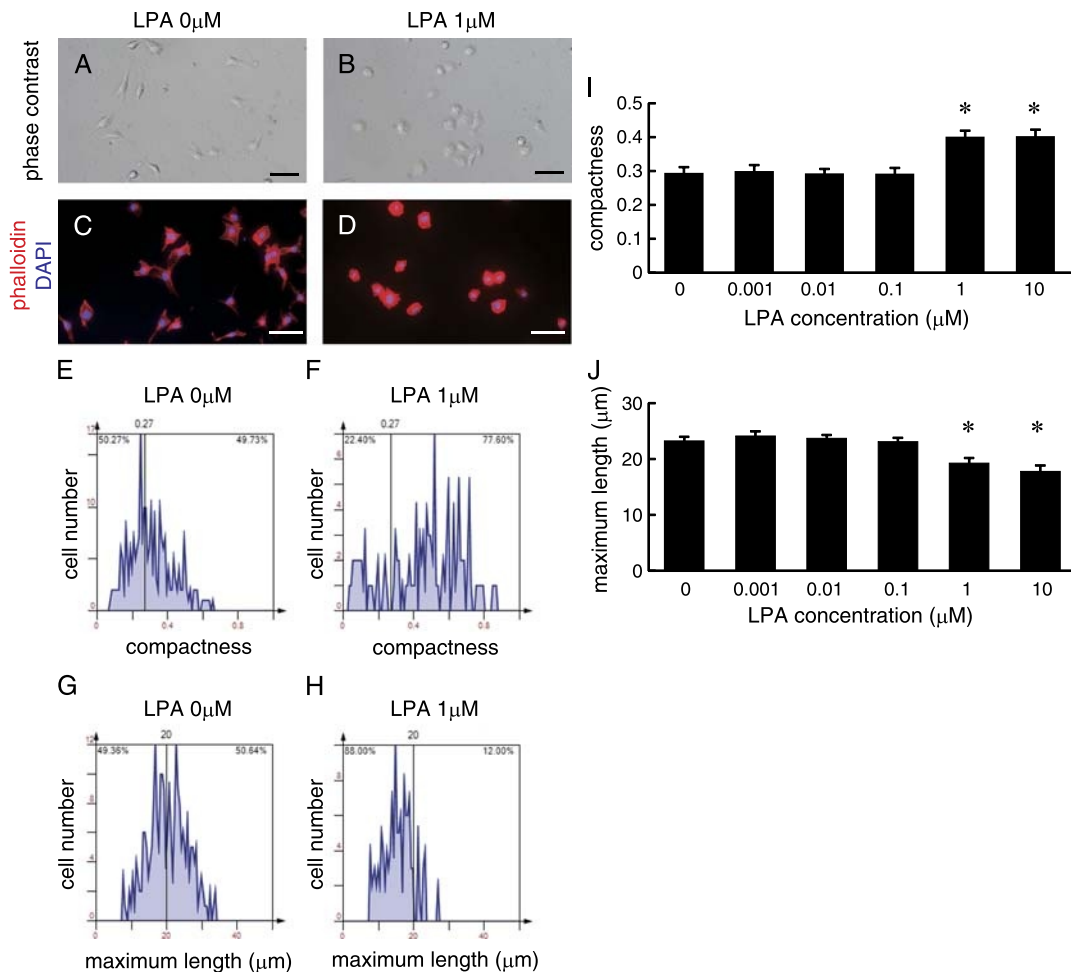
FIGURE 4. The inhibition of spreading of BEAS-2B cells by LPA. A, B, Phase contrast images of BEAS-2B on the tissue culture plate, incubated with or without LPA for 1.5 hours. C, D, Phalloidin staining of BEAS-2B after 1.5 hours of incubation with or without LPA. Bars = 50 μm. E, F, Representative histogram of cell compactness, as analyzed by TissueFAXS after 1.5 hours of incubation with or without LPA. The closer the value of compactness to 1 the more compacted the cell shape. Each area of the histogram is divided by a value of 0.27 at the horizontal axis, which is the average of the compactness of LPA 0 μM. The percentage in each area indicates the ratio of the cell number in the areas. G, H, A representative histogram of the maximum cell length, as analyzed by TissueFAXS after 1.5 hours incubation with or without LPA. Each area is divided by 20 at the horizontal axis, which is the average of the maximum length of LPA 0 μM. The percentage in each area indicates the ratio of the cell number in the area. I, The compactness of BEAS-2B after 1.5 hours of incubation with various concentration of LPA. J, The maximum length of BEAS-2B after 1.5 hours of incubation with various concentration of LPA. The data are expressed as the mean + SEM (n = 7). *$P < 0.05$ versus LPA 0 μM.

Y27632. In addition, the maximum cell length was increased with Y27632 to the same level as without LPA (Figure 7F). These results indicate that LPA signaling via LPA_1 is involved in Rho-kinase pathway.

The Inhibition of Epithelial Cell Loss in the Heterotopically Transplanted Tracheal Allograft by an LPA_1- and LPA_3-Specific Antagonist Is not Continued to the Later Phase

To examine whether LPA signaling via LPA_1 and/or LPA_3 involved in the onset of obliteration, the allografts harvested at 28 days after transplantation were also assessed (Figure 8) (**Figure S2, SDC,** http://links.lww.com/TXD/A10). Different from day 10, the loss of airway epithelial cells was severe in the Ki16198-treated allografts compared with the vehicle-treated grafts (Figures 8A-E). Leukocyte infiltration, ECM deposition, and luminal obliteration were not significantly changed between the vehicle and Ki16198-treated allografts,

whereas all of these scores increased compared with those at day 10 (Figures 8F, G, H).

Unexpectedly, we observed that the epithelial cells of Ki16198-treated allografts harvested at 28 days were severely denuded from the basement membrane compared with those of vehicle-treated allograft. Babu et al[17] demonstrated that prevention of microvascular destruction is important for epithelial cell loss and consequently fibrosis. Because LPA induce vascularization,[18] we hypothesized that inhibition of the LPA signaling via LPA_1 and LPA_3 might suppress vascularization within the allograft, and it might cause epithelial cell denudation in the Ki16198-treated allografts in longer time course after the transplantation. Antibody against CD31, an endothelial cell marker protein, detected immunoreactive cells in both vehicle- and Ki16198-treated grafts. However, although CD31-positive cells form vascular structure in the vehicle-treated graft, many of CD31-positive cells did not form vascular structure and were solely located in Figures 9A, B. The number of CD31-positive vascular
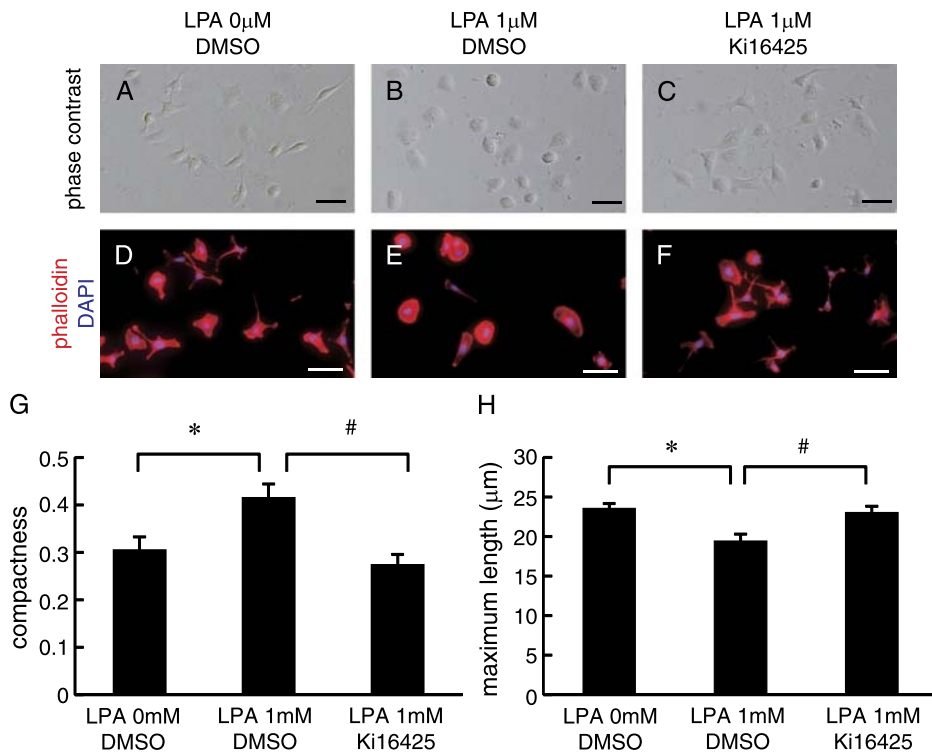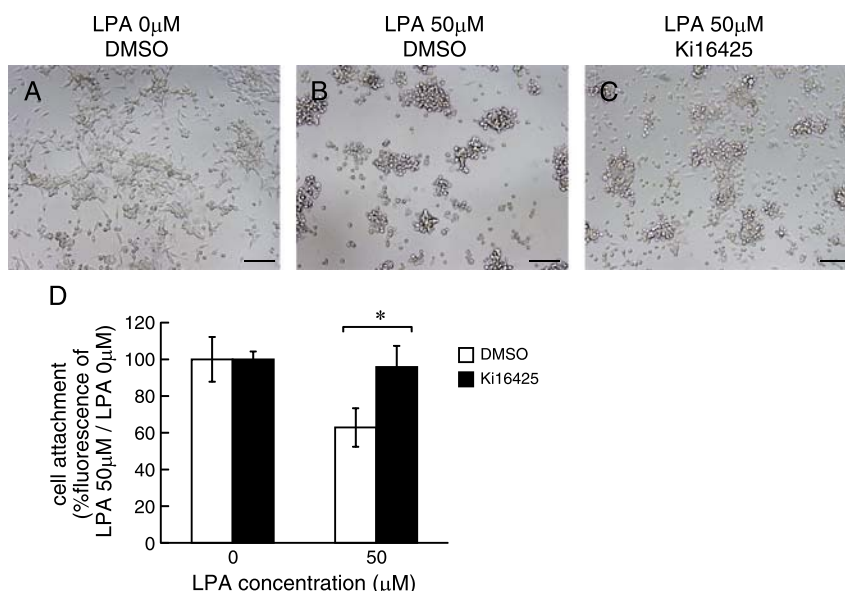
FIGURE 5. Restoration of inhibition of BEAS-2B cell spreading by LPA by the addition of Ki16425. A-C, Phase contrast images of BEAS-2B on the tissue culture plate following incubation with the indicated combinations of LPA, DMSO, or Ki16425 for 1.5 hours. D-F, Phalloidin staining of BEAS-2B after 1.5 hours of incubation with the indicated combinations of LPA, DMSO, or Ki16425. Bars = 50 μm. G, The compactness of BEAS-2B after 1.5 hours of incubation with the indicated combinations of LPA, DMSO, or Ki16425. H, The maximum length of BEAS-2B after 1.5 hours of incubation with the indicated combinations of LPA, DMSO, or Ki16425. The data are expressed as the mean + SEM (n = 4). *$P < 0.05$ LPA 0 μM and DMSO versus LPA 1 μM and DMSO, #$P < 0.05$ LPA 1 μM and DMSO versus LPA 1 μM and Ki16425.

structure of Ki16198-treated graft was smaller than that of vehicle-treated graft (Figure 9C).

DISCUSSION

In the present study, we found that an $LPA_1/_3$-specific antagonist attenuates the loss of airway epithelial cells in a heterotopic tracheal transplantation mouse allograft model at an early phase, but its effect is not continued and obliteration is not prevented by a later phase. The LPA_1 and LPA_3 were expressed in the mouse airway epithelial cells. We revealed that the addition of LPA to human airway epithelial cell culture resulted in the prevention of cell attachment to

FIGURE 6. Induction of BEAS-2B detachment from the low attachment plate with LPA and the inhibition of cell detachment the addition of Ki16425. A-C, Phase contrast images of BEAS-2B on the nontissue culture assay plate following incubation with the indicated combinations of LPA, DMSO, or Ki16425 for 6 hours. Bars = 100 μM. D, The detachment of BEAS-2B after 6 hours of incubation with the indicated combinations of LPA, DMSO, or Ki16425. The data are expressed as the mean ± SEM (n = 3), *$P < 0.05$.
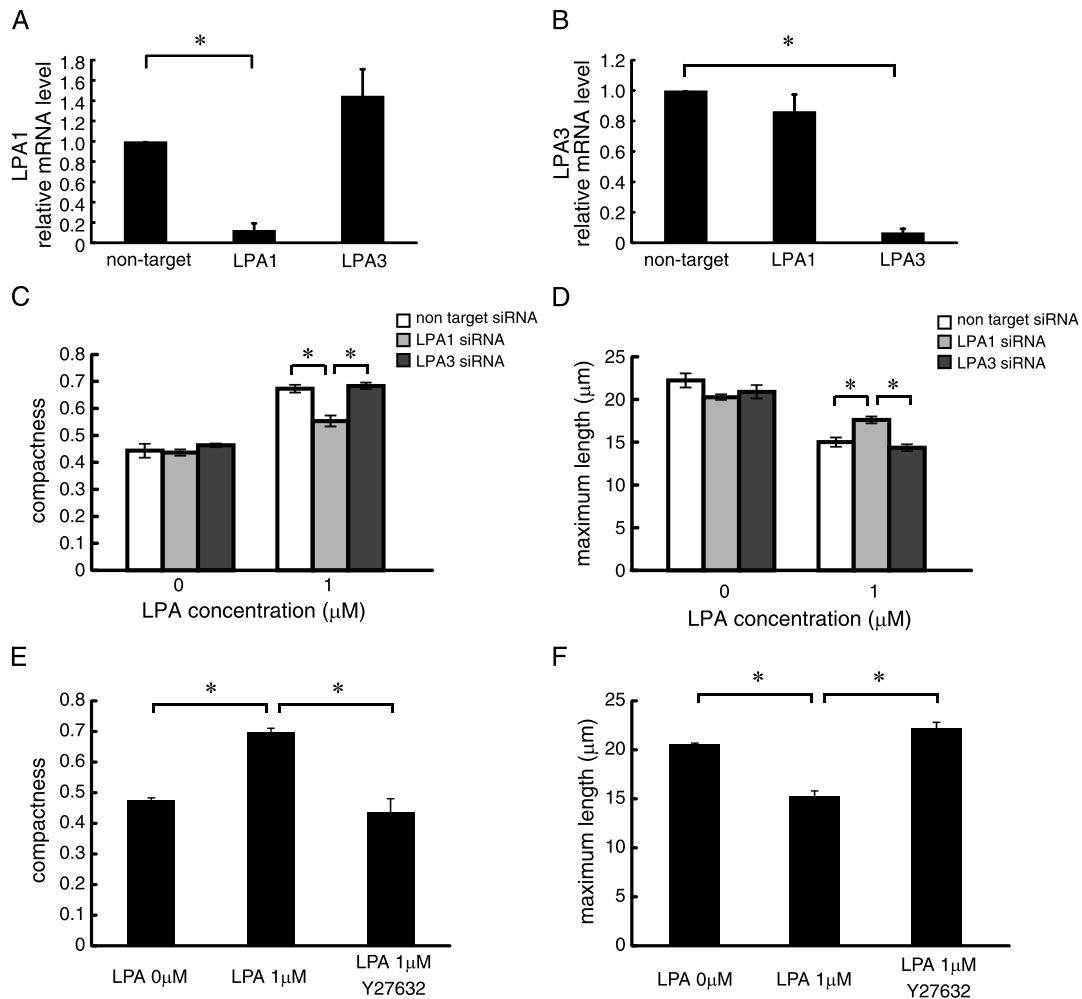
FIGURE 7. Involvement of LPA$_1$ and Rho-kinase signaling on BEAS-2B cell spreading. Messenger RNA for LPA$_1$ (A) or LPA$_3$ (B) after transfection of siRNA for LPA$_1$ or LPA$_3$ were significantly decreased compared with its expression in cells transfected with control non-target siRNA, respectively. Relative mRNA level in the nontarget siRNA was indicated as 1. The compactness of LPA$_1$ siRNA transfected BEAS-2B was decreased (C), and the maximum cell length of these cells were increased (D) compared with nontarget siRNA and LPA$_3$ siRNA, respectively after 1.5 hours of incubation with 1 µM of LPA. E, The compactness of BEAS-2B after 1.5 hours of incubation with the indicated combinations of LPA or Y27632. F, The maximum length of BEAS-2B after 1.5 hours of incubation with the indicated combinations of LPA or Y27632. The data are expressed as the mean ± SEM (n = 3), *$P < 0.05$.

the ECM, and its intracellular signaling is mediated by LPA$_1$ and Rho-kinase signaling.

We found many remaining airway epithelial cells on the basement membrane in the allografts from Ki16198-administered mice compared with the control allografts at day 10 after the transplantation. We also observed that the number of TUNEL-positive epithelial cells was decreased in Ki16198-treated grafts. Contrary to our results, in most circumstances, LPA increased cell viability through suppression of apoptosis.[6] However, the induction of apoptosis by LPA was observed in neurons[19,20] and normal human bronchial epithelial (NHBE) cells,[21] and this study, suggesting that the effect of LPA against apoptosis may differ among cell types. A previous study reported that apoptosis of epithelial cells occurred in tracheal transplantation animal models.[22,23] Apoptosis in the epithelial cells is also found in the airway of patients with OB.[24] These studies demonstrate the contribution of apoptosis to the damage of epithelial cells during the progression of OB. On the other hand, we observed that the epithelial cells of the allograft from Ki16198-administrated mice severely denuded at day 28. We also found the number of CD31

immunoreactive vascular structure is smaller in the Ki16198-treated graft compared with vehicle-treated graft. Because functional microvascularization after transplantation is important in the prevention of epithelial cell loss,[17] and inhibition of LPA signaling block vascularization,[18] poor vascularization observed in Ki16198-treated graft might come from inhibition of LPA signaling by the treatment of Ki16198. However, there are several limitations of heterotopic tracheal transplantation model used in this study due to different external environment from the thoracic milieu, while it is highly accessible and reproducible model. To reveal more precise role of LPA in the OB lesion, the experiments using orthotopic tracheal transplantation, which is a more representative model of OB,[25] would be desirable. Taken together, our results suggest that LPA signaling via LPA$_1$ and LPA$_3$ contributes to the denudation of airway epithelial cells at early phase, but not the suppression of vascularization of the graft at a later phase in an alloimmune environment.

Several studies have demonstrated that airway epithelial cells can serve as immunological targets during the process
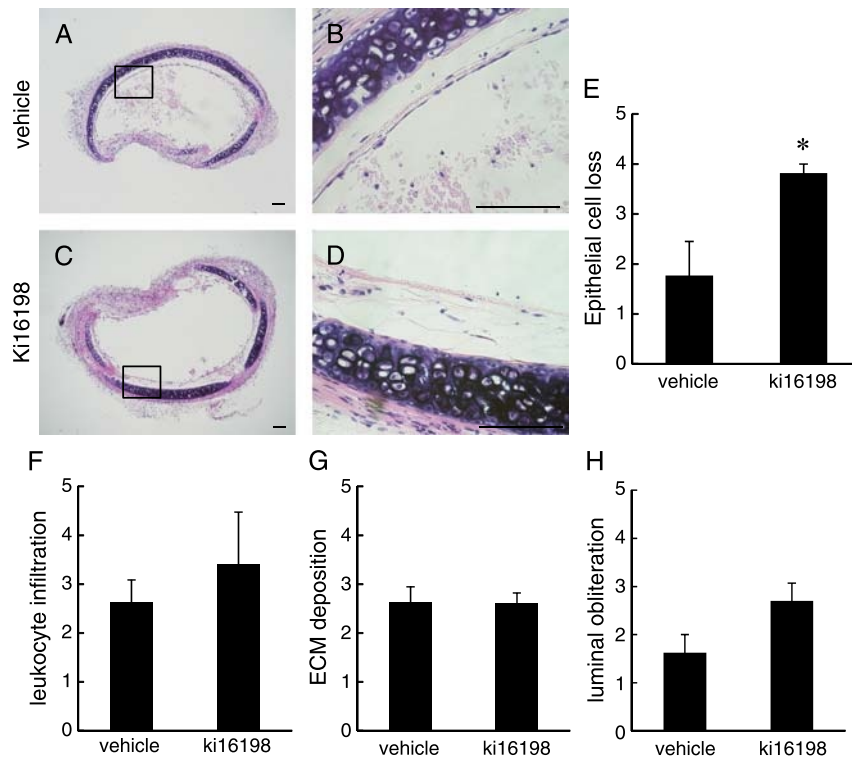
FIGURE 8. The graft histology of vehicle or Ki16198-treated mouse on day 28. A-D, Representative hematoxylin-eosin staining of the transverse section of vehicle or Ki16198-treated mouse tracheal heterotopic transplanted allograft at 28 days. The airway epithelial cells are preserved in the graft from a vehicle-treated mouse (A, B) rather than Ki16198-treated mouse (C, D). The areas surrounded by squares in (A) and (C) are magnified in (B) and (D), respectively. Bars = 100 μm. E, The histopathologic score (0 = normal, 1 = mild, 2 = moderate, 3 = severe, and 4 = very severe damage) of the vehicle- or Ki16198-treated mouse tracheal epithelial cell loss (E), leukocyte infiltration (F), ECM deposition (G), and luminal obliteration (H). The data are expressed as the mean + SEM (n = 7 for vehicle, n = 8 for Ki16198). The data are expressed as the mean + SEM (n = 7 for vehicle, n = 8 for Ki16198), *$P < 0.05$.
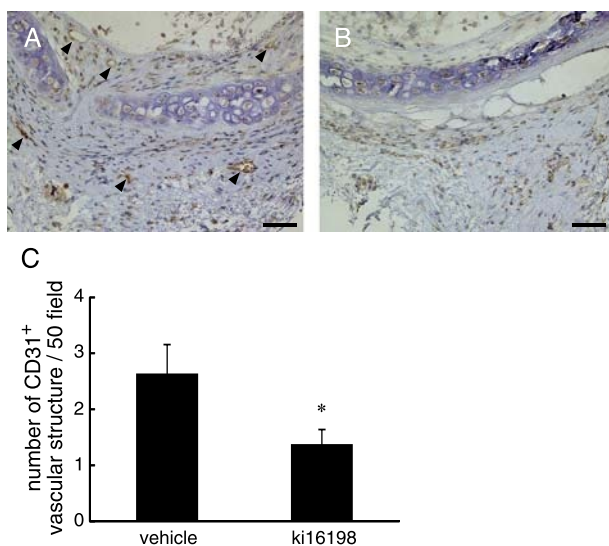
FIGURE 9. Detection of endothelial cells for vehicle- or Ki16198-treated mouse allografts on day 28. CD31 antibody detected clear vascular structure in vehicle-treated allograft section (A, arrows), while only dot-like pattern of CD31 immunoreactivity was detected in Ki16198-treated allograft section (B). Bars = 50 μm. (C) Quantification of CD31 positive vascular structure. The number of vascular structure located at outside of the cartilage was counted in randomly selected 50 fields from each section of vehicle- or Ki16198- treated allograft with 40 times objective lens. The data are expressed as the mean ± SEM (n = 50). *$P < 0.05$.

of lung allograft rejection. Airway epithelial cells are able to express major histocompatibility complex class II molecules, and this expression is upregulated during chronic allograft rejection.[26] In addition, cytotoxic T lymphocytes directed against HLA class I antigens of donor airway epithelial cell have been found in patients with OB.[27] On the other hand, it has been reported that LPA is a chemoattractant for multiple leukocyte subsets.[28,29] However, our in vivo experiment with Ki16198 did not alter leukocyte infiltration in the allografts. Therefore, LPA signaling through LPA$_1$ or LPA$_3$ does not contribute to leukocyte chemotaxis in this animal model. Furthermore, we found that the mRNA of both LPA$_1$ and LPA$_3$ were expressed in the airway epithelial cells, although the protein localization of these receptors by immunohistochemistry was not possible due to the insufficient specificity and sensitivity of the available antibodies. We found that LPA$_2$ and LPA$_6$ were also expressed in airway epithelial cells. Although the role of LPA$_6$ in the airway has not been established, LPA$_2$ has been reported to have a role in the development of allergic airway inflammation in a murine model of asthma.[30] Thus, different LPA signaling via different LPA receptors might be involved in the various pathologies of the airway epithelial cells.

We also observed that LPA inhibits the spreading of BEAS-2B cells to the ECM and induces cell detachment from the ECM, which indicates that LPA reduces BEAS-2B cell adhesion to the ECM. The disruption of the interaction between epithelial cells and the ECM results in cell apoptosis.[31] Although apoptosis has been reported to occur in NHBE cells

treated with LPA,[21] we did not observe apoptosis in BEAS-2B cells exposed to LPA, even after cell attachment was reduced (data not shown). These different results might be due to the different robustness of these cells. Although NHBE cells are freshly isolated from human lungs, BEAS-2B cells are immortalized cells derived from normal human bronchial epithelium. Therefore, LPA stimulation might not be enough to induce apoptosis in BEAS-2B cells while cell attachment is decreased. Furthermore, we demonstrated that the BEAS-2B cell attachment regulation by LPA is mediated by LPA_1 and Rho-kinase. Because LPA signaling via LPA_1 and Rho-kinase pathway induce cytoskeletal change,[32] decrease of cell attachment might be suppressed due to modification of cell shape. Taken together, the results of this study strongly support the role of LPA in the regulation of cell adhesion in bronchial epithelial cells.

In the current study, we revealed the involvement of LPA signaling in a mouse model of OB. This finding indicates that LPA signaling is activated in an alloimmune environment. How is LPA signaling activated? Nakasaki et al[33] reported that autotaxin (ATX), the major LPA-generating ectoenzyme that converts lysophosphatidylcholine to LPA, is expressed in the venules and plays a role in lymphocyte trafficking to chronically inflamed tissues. Tissue inflammation of the allograft due to alloimmune reactions is a principal phenomenon observed in allotransplantation. Accordingly, human OB is characterized by chronic inflammation of the bronchial epithelium.[34] Based on these reports, the following scenario of LPA signaling activation in airway epithelial cells is possible: (1) The ATX is secreted from chronically inflamed tissues after allotransplantation. (2) The LPA is generated from lysophosphatidylcholine by ATX. (3) The LPA binds to LPA receptors located on the target cells in the allograft, and LPA signaling is activated within the cells. To reveal the precise mechanism of LPA signaling activation, the measurement of LPA concentration in the bronchoalveolar lavage of OB patients, as well as ATX expression in the tissue samples isolated from OB patients, needs to be investigated.

The possibility that LPA has the other roles for the onset of OB in addition to this study cannot be excluded. The LPA activates secretion of inflammatory cytokine IL-8 in human bronchial epithelial cells.[35] Therefore, the effect of LPA on the epithelial cells might be involved in the inflammation after lung transplantation. The role of LPA except for the epithelial cells is also possible. The LPA has been shown to induce the migration of lung fibroblasts.[9] Fibroblast and circulating fibroblast precursor cells, termed fibrocytes, have been reported to be involved in the onset of OB lesions.[36,37] In addition, LPA also induces the migration of lung-resident mesenchymal stem cells[38] and bone marrow-derived mesenchymal stem cells,[39] a process that is also involved in OB.[40,41] Further research on the involvement of these cells in the onset of OB will be the subject of future investigations.

CONCLUSIONS

We demonstrated that LPA signaling is involved in the status of epithelial cells by distinct contribution in 2 different phases of the OB lesion: (1) loss of airway epithelial cells in the early phase through inhibition of cell attachment to the ECM, and (2) re-epithelialization in the later phase by promoting vascularization of the graft. Our study suggests LPA signaling as a potential novel therapeutic target for the prevention of OB at the early phase after the transplantation.

REFERENCES

1. Trulock EP, Christie JD, Edwards LB, et al. Registry of the International Society for Heart and Lung Transplantation: twenty-fourth official adult lung and heart-lung transplantation report-2007. *J Heart Lung Transplant*. 2007; 26:782–795.
2. Boehler A, Kesten S, Weder W, et al. Bronchiolitis obliterans after lung transplantation: a review. *Chest*. 1998;114:1411–1426.
3. Estenne M, Hertz MI. Bronchiolitis obliterans after human lung transplantation. *Am J Respir Crit Care Med*. 2002;166:440–444.
4. Belperio JA, Weigt SS, Fishbein MC, et al. Chronic lung allograft rejection: mechanisms and therapy. *Proc Am Thorac Soc*. 2009;6:108–121.
5. Moolenaar WH. Lysophosphatidic acid, a multifunctional phospholipid messenger. *J Biol Chem*. 1995;270:12949–12952.
6. Mills GB, Moolenaar WH. The emerging role of lysophosphatidic acid in cancer. *Nat Rev Cancer*. 2003;3:582–591.
7. Yung YC, Stoddard NC, Chun J. LPA receptor signaling: pharmacology, physiology, and pathophysiology. *J Lipid Res*. 2014;55:1192–1214.
8. Pradère JP, Klein J, Grès S, et al. LPA1 receptor activation promotes renal interstitial fibrosis. *J Am Soc Nephrol*. 2007;18:3110–3118.
9. Tager AM, LaCamera P, Shea BS, et al. The lysophosphatidic acid receptor LPA1 links pulmonary fibrosis to lung injury by mediating fibroblast recruitment and vascular leak. *Nat Med*. 2008;14:45–54.
10. Swaney JS, Chapman C, Correa LD, et al. A novel, orally active LPA(1) receptor antagonist inhibits lung fibrosis in the mouse bleomycin model. *Br J Pharmacol*. 2010;160:1699–1713.
11. Hertz MI, Jessurun J, King MB, et al. Reproduction of the obliterative bronchiolitis lesion after heterotopic transplantation of mouse airways. *Am J Pathol*. 1993;142:1945–1951.
12. Hele DJ, Yacoub MH, Belvisi MG. The heterotopic tracheal allograft as an animal model of obliterative bronchiolitis. *Respir Res*. 2001;2:169–183.
13. Komachi M, Sato K, Tobo M, et al. Orally active lysophosphatidic acid receptor antagonist attenuates pancreatic cancer invasion and metastasis in vivo. *Cancer Sci*. 2012;103:1099–1104.
14. Belperio JA, Keane MP, Burdick MD, et al. Critical role for CXCR3 chemokine biology in the pathogenesis of bronchiolitis obliterans syndrome. *J Immunol*. 2002;169:1037–1049.
15. Matsuzaki S, Ishizuka T, Hisada T, et al. Lysophosphatidic acid inhibits CC chemokine ligand 5/RANTES production by blocking IRF-1-mediated gene transcription in human bronchial epithelial cells. *J Immunol*. 2010; 185:4863–4872.
16. Ohta H, Sato K, Murata N, et al. Ki16425, a subtype-selective antagonist for EDG-family lysophosphatidic acid receptors. *Mol Pharmacol*. 2003; 64:994.
17. Babu AN, Murakawa T, Thurman JM, et al. Microvascular destruction identifies murine allografts that cannot be rescued from airway fibrosis. *J Clin Invest*. 2007;117:3774–3785.
18. Rivera-Lopez CM, Tucker AL, Lynch KR. Lysophosphatidic acid (LPA) and angiogenesis. *Angiogenesis*. 2008;11:301–310.
19. Holtsberg FW, Steiner MR, Keller JN, et al. Lysophosphatidic acid induces necrosis and apoptosis in hippocampal neurons. *J Neurochem*. 1998;70:66–76.
20. Holtsberg FW, Steiner MR, Bruce-Keller AJ, et al. Lysophosphatidic acid and apoptosis of nerve growth factor-differentiated PC12 cells. *J Neurosci Res*. 1998;53:685–696.
21. Funke M, Zhao Z, Xu Y, et al. The lysophosphatidic acid receptor LPA1 promotes epithelial cell apoptosis after lung injury. *Am J Respir Cell Mol Biol*. 2012;46:355–364.
22. Neuringer IP, Aris RM, Burns KA, et al. Epithelial kinetics in mouse heterotopic tracheal allografts. *Am J Transplant*. 2002;2:410–419.
23. Alho HS, Salminen US, Maasilta PK, et al. Epithelial apoptosis in experimental obliterative airway disease after lung transplantation. *J Heart Lung Transplant*. 2003;22:1014–1022.
24. Hansen PR, Holm AM, Svendsen UG, et al. Apoptosis and formation of peroxynitrite in the lungs of patients with obliterative bronchiolitis. *J Heart Lung Transplant*. 2000;19:160–166.
25. Deuse T, Schrepfer S, Reichenspurner H, et al. Techniques for experimental heterotopic and orthotopic tracheal transplantations—when to use which model? *Transpl Immunol*. 2007;17:255–261.

26. Milne DS, Gascoigne AD, Wilkes J, et al. MHC class II and ICAM-1 expression and lymphocyte subsets in transbronchial biopsies from lung transplant recipients. *Transplantation*. 1994;57:1762–1766.

27. Nakajima J, Poindexter NJ, Hillemeyer PB, et al. Cytotoxic T lymphocytes directed against donor HLA class I antigens on airway epithelial cells are present in bronchoalveolar lavage fluid from lung transplant recipients during acute rejection. *J Thorac Cardiovasc Surg*. 1999;117:565–571.

28. Hashimoto T, Yamashita M, Ohata H, et al. Lysophosphatidic acid enhances in vivo infiltration and activation of guinea pig eosinophils and neutrophils via a Rho/Rho-associated protein kinase-mediated pathway. *J Pharmacol Sci*. 2003;14:8–14.

29. Kehrl JH. Signaling and the control of lymphocyte migration. *Immunol Res*. 2006;34:211.

30. Zhao Y, Tong J, He D, et al. Role of lysophosphatidic acid receptor LPA2 in the development of allergic airway inflammation in a murine model of asthma. *Respir Res*. 2009;10:114.

31. Frisch SM, Francis H. Disruption of epithelial cell-matrix interactions induces apoptosis. *J Cell Biol*. 1994;124:619–626.

32. Mutoh T, Rivera R, Chun J. Insights into the pharmacological relevance of lysophospholipid receptors. *Br J Pharmacol*. 2012;165:829–844.

33. Nakasaki T, Tanaka T, Okudaira S, et al. Involvement of the lysophosphatidic acid-generating enzyme autotaxin in lymphocyte-endothelial cell interactions. *Am J Pathol*. 2008;173:1566–1576.

34. McDyer JF. Human and murine obliterative bronchiolitis in transplant. *Proc Am Thorac Soc*. 2007;4:37–43.

35. Zhao Y, Usatyuk PV, Cummings R, et al. Lipid phosphate phosphatase-1 regulates lysophosphatidic acid-induced calcium release, NF-kappaB activation and interleukin-8 secretion in human bronchial epithelial cells. *Biochem J*. 2005;385(Pt 2):493–502.

36. Bröcker V, Länger F, Fellous TG, et al. Fibroblasts of recipient origin contribute to bronchiolitis obliterans in human lung transplants. *Am J Respir Crit Care Med*. 2006;173:1276–1282.

37. Andersson-Sjöland A, Erjefält JS, Bjermer L, et al. Fibrocytes are associated with vascular and parenchymal remodelling in patients with obliterative bronchiolitis. *Respir Res*. 2009;10:103.

38. Badri L, Lama VN. Lysophosphatidic acid induces migration of human lung-resident mesenchymal stem cells through the β-catenin pathway. *Stem Cells*. 2012;30:2010–2019.

39. Tang N, Zhao Y, Feng R, et al. Lysophosphatidic acid accelerates lung fibrosis by inducing differentiation of mesenchymal stem cells into myofibroblasts. *J Cell Mol Med*. 2014;18:156–169.

40. Badri L, Murray S, Liu LX, et al. Mesenchymal stromal cells in bronchoalveolar lavage as predictors of bronchiolitis obliterans syndrome. *Am J Respir Crit Care Med*. 2011;183:1062–1070.

41. Walker N, Badri L, Wettlaufer S, et al. Resident tissue-specific mesenchymal progenitor cells contribute to fibrogenesis in human lung allografts. *Am J Pathol*. 2011;178:2461–2469.